Trace gas fluxes from tidal salt marsh soils: implications for carbon-sulfur biogeochemistry

Margaret Capooci[1] and Rodrigo Vargas [1*]

[1] Department of Plant and Soil Science
University of Delaware
152 Townsend Hall
531 South College Ave.
Newark, DE, USA 19716

* *Correspondence to:*
Rodrigo Vargas
152 Townsend Hall
531 South College Ave.,
Newark, DE 19716
rvargas@udel.edu
Phone: 302-831-1386

Abstract

Tidal salt marsh soils can be a dynamic source of greenhouse gases such as carbon dioxide (CO_2), methane (CH_4), and nitrous oxide (N_2O), as well as sulfur-based trace gases such as carbon disulfide (CS_2) and dimethylsulfide (DMS) which play roles in global climate and carbon-sulfur biogeochemistry. Due to the difficulty in measuring trace gases in coastal ecosystems (e.g., flooding, salinity), our current understanding is based on snap-shot instantaneous measurements (e.g., performed during daytime low tide) which complicates our ability to assess the role of these ecosystems for natural climate solutions. We performed continuous, automated measurements of soil trace gas fluxes throughout the growing season to obtain high-temporal frequency data and to provide insights into magnitudes and temporal variability across rapidly changing conditions such as tidal cycles. We found that soil CO_2 fluxes did not show a consistent diel pattern, CH_4, N_2O, and CS_2 fluxes were highly variable with frequent pulse emissions (>2,500%, >10,000%, and >4,500% change, respectively), and DMS fluxes only occurred mid-day with changes >185,000%. When we compared continuous measurements with discrete temporal measurements (during daytime, at low tide), discrete measurements of soil CO_2 fluxes were comparable with those from continuous measurements, but misrepresent the temporal variability and magnitudes of CH_4, N_2O, DMS, and CS_2. Discrepancies between the continuous and discrete measurement data result in differences for calculating the sustained global warming potential (SGWP), mainly by an overestimation of CH_4 fluxes when using discrete measurements. The high temporal variability of trace gas fluxes complicates the accurate calculation of budgets for use in blue carbon accounting and earth system models.

1. Introduction

Coastal vegetated ecosystems such as tidal salt marshes, mangrove forests, and seagrass beds provide a wide range of ecosystem services, such as mitigating storm surge and providing nursery areas for fish species (Barbier et al., 2011; Möller et al., 2014). They also can potentially store large amounts of carbon at rates forty times higher than tropical rainforests (Rosentreter et al., 2018; Duarte et al., 2005) and are referred to as "blue carbon" ecosystems. The importance of coastal vegetated ecosystems in climate change policies has been recognized by the Paris Agreement (UNFCCC, 2015). Prior to the Paris Agreement, there has been increased interest in better quantifying the net balance between carbon storage and carbon release in coastal vegetated ecosystems for both scientific and carbon market purposes. For example, the Verified Carbon Standard developed a methodology to assess and verify the amount of carbon removed from the atmosphere in tidal wetland and seagrass restoration projects for carbon market purposes (Emmer et al., 2021). However, there are major knowledge gaps in assessing blue carbon in coastal vegetated ecosystems. Specifically, the high spatial and temporal variability of greenhouse gas (GHG) emissions, particularly for CH_4 and N_2O, in coastal vegetated ecosystems complicates blue carbon offset calculations (Rosentreter et al., 2021; Capooci et al., 2019; Al-Haj and Fulweiler, 2020; Murray et al., 2015). Thus, there is a need for developing measurement protocols to fully quantify the contribution of multiple GHGs in blue carbon ecosystems.

To improve our understanding of blue carbon ecosystems in global biogeochemical cycles we need to think beyond traditional GHG trace gases (i.e., CO_2, CH_4, N_2O). Tidal salt marshes produce sulfur-based trace gases due to the prevalence of sulfur cycling within their soils, which has implications for carbon-sulfur biogeochemistry and the global climate. While coastal areas are major sources of sulfur gases (Kellogg et al., 1972), there is large

uncertainty in emission rates (Carroll et al., 1986; Andreae and Jaeschke, 1992; Brimblecombe, 2014). Dimethyl sulfide (DMS) is one of the dominant sulfur-based gases emitted from salt marshes (Hines, 1996) and is considered a climate cooling gas, in part due to its oxidation to SO_4 in the atmosphere (Thomas et al., 2010; Watts, 2000; Charlson et al., 1987). Dimethylsulfoniopropionate (DMSP), a DMS precursor, can be produced by salt marsh plant species *Spartina alterniflora*, *S. anglica*, and *S. foliosa* (Hines, 1996). DMS plays an important role in linking together carbon and sulfur biogeochemistry in salt marsh soils. It can be decomposed by not only sulfate-reducing bacteria, but can also act as a non-competitive substrate for methylotrophic methanogenesis (Kiene, 1988; Kiene and Visscher, 1987; Oremland et al., 1982) which allows methane production to occur in soils dominated by sulfate reduction (Seyfferth et al., 2020). Another sulfur-based trace gas released from tidal salt marshes is carbon disulfide (CS_2), which has an insignificant global warming potential and a short atmospheric lifetime (Brühl et al., 2012). However, CS_2 is a precursor to carbonyl sulfide (COS; Whelan et al., 2013). COS is the most abundant reduced sulfur compound in the atmosphere and can form sulfate aerosols that affect the Earth's radiative properties by reflecting sunlight, thereby having a cooling effect on the climate (Watts, 2000; Taubman and Kasting, 1995). Despite sulfur-based trace gases playing a role in wetland soil biogeochemistry and in global climate, there is a need to quantify coastal wetland sulfur emissions and to connect those emissions to both the salt marsh sulfur cycle and to global budgets (DeLaune et al., 2002; Whelan et al., 2013).

Historically, both soil GHGs and S-based fluxes are measured using manual survey chambers, particularly during daytime low tide (e.g., De Mello et al., 1987) when soils are less likely to be submerged and are accessible to researchers. Measurements at high tide in salt marshes are difficult due to both reduced access to the marsh platform and reduced fluxes. Gases

from the soil mix with the overlying water column and move more slowly through water compared to air, contributing to a decline in fluxes during high tide (Moffett et al., 2010). Manual measurements have a number of advantages, including the ability to sample over large areas over short periods of time (Moseman-Valtierra et al., 2016; Simpson et al., 2019), but these measurements are labor-intensive and provide limited information regarding temporal variability (Koskinen et al., 2014; Savage et al., 2014; Vargas et al., 2011). On the other hand, recent advances in high temporal-frequency soil efflux measurements (Capooci and Vargas, 2022; Diefenderfer et al., 2018; Järveoja et al., 2018) have provided researchers with unprecedented temporal information to better understand diel and tidal patterns, as well as the influence of pulse events on trace gas emissions within salt marshes. While the use of automated systems is becoming more common in measuring salt marsh fluxes (Capooci and Vargas, 2022; Diefenderfer et al., 2018; Trifunovic et al., 2020), their use is limited by high instrumentation costs, electricity requirements, and logistical challenges associated with installing these instruments in an environment prone to flooding and with high humidity. As automated systems become more prevalent, it provides researchers with the opportunity to evaluate data collected from manual measurements, such as daily means, that have been used to inform models and budgets, particularly for understudied trace gases such as N_2O, CS_2, and DMS.

The objective of this study is to characterize the spatial and temporal variability of trace gases from soils in a tidal salt marsh. Specifically, we focus on CO_2, CH_4, N_2O, CS_2, and DMS to assess the differences between measurements taken at a particular time of day (i.e., daytime low tide) and measurements with high-temporal frequency (i.e., continuous hourly measurements for ~72 hours). Few studies have measured GHG fluxes from tidal salt marshes using continuous, automated measurements (Diefenderfer et al., 2018; Capooci and Vargas, 2022), and

this is a pioneering study that provides unprecedented information about the magnitudes and patterns of CS_2 and DMS fluxes via continuous measurements. Furthermore, this study tests whether traditional measurement protocols based on discrete temporal measurements provide similar information as data derived from continuous measurements, including the calculation of the sustained global warming potential (SGWP). Development of new technologies and incorporation of this information has important implications for calculating greenhouse and trace gas budgets, as well as the role salt marshes play in global biogeochemical cycles.

2. Materials and methods

2.1 Study site

The study was conducted at St. Jones Reserve, the brackish estuarine component of the Delaware National Estuarine Research Reserve. The site is part of the Delaware Estuary and is tidally connected to the Delaware Bay via the St. Jones River. St. Jones is classified as a mesohaline tidal salt marsh (DNREC, 1999) and has silty clay loam soils (10% sand, 61% silt, 29% loam, Capooci et al 2019). The study was conducted in a section of the marsh dominated by *Spartina alterniflora* (= *Sporobolus alterniflorus* (Loisel.); Peterson et al., 2014) and will be referred to as SS as established in previous studies (Seyfferth et al., 2020; Capooci and Vargas, 2022). This area is lower in elevation relative to the rest of the marsh, is characterized by sulfur reduction (Seyfferth et al., 2020), and covers ~66% of the salt marsh landscape (Vázquez-Lule and Vargas, 2021). The SS site rarely floods during high tide due to its distance from the tidal creek (~50 m), as well as the presence of a berm located adjacent to the tidal creek (Seyfferth et., 2020; Hill et al., 2021).

134

135 *2.2 Experimental set-up*

136 The experiment was performed over the course of 6 campaigns to cover a full growing
137 season: greenup (G), maturity (M), senescence (S), and dormancy (D) as described by the
138 canopy phenology of the study site (Hill et al., 2021). The campaigns began during the latter half
139 of the 2020 growing season and continued into beginning of the 2021 growing season (M1 – 29
140 June to 2 July, M2 – 31 July to 3 Aug, S1 – 31 Aug to 3 Sept, S2 – 28 Sept to 1 Oct, D1 – 13
141 Apr to 16 Apr, and G1 – 31 May to 3 June) due to delays related to the COVID-19 pandemic.
142 We installed six PVC collars (diameter: 20 cm), placed ~1.2 meters apart, four months prior to
143 the beginning of the experiment in the year 2020. Collars were placed in a *S. alterniflora* area of
144 the marsh near the boardwalk to minimize impacts to the marsh, as well as to easily access
145 boardwalk power outlets. Any vegetation that grew inside these collars in between campaigns
146 was carefully clipped at the base of the stem prior to each campaign. Vegetation was clipped on a
147 frequent basis to minimize stem diameters and thereby reduced the effects of plant-mediated gas
148 transport. These collars were used to set down six opaque automated chambers (LICOR 8100-
149 104, Lincoln, Nebraska; volume: 4071.1 cm^3) to measure trace gas fluxes as described below.

150

151 *2.3 Trace gas flux measurements and QA/QC*

152 The autochambers were coupled with a closed-path infrared gas analyzer (LI-8100A,
153 LICOR, Lincoln, Nebraska) and a Fourier transform infrared spectrometer (DX4040, Gasmet
154 Technologies Oy, Vantaa, Finland). The LI-8100A and the DX4040 were connected in parallel
155 since the DX4040 has its own internal pump and flow rates. Trace gas fluxes were measured
156 once per hour per chamber (i.e., all six chambers were measured within an hour). Measurements

were 5 minutes long and each chamber was flushed for 5 minutes total (pre-purge and post-purge were both 2.5 minutes long) to help reduce the impacts of humidity on the instruments. Each campaign lasted approximately 72 hours where approximately 416 measurements were recorded. Campaigns were short in length due to electrical power limitations and to minimize instrumentation damage due to the corrosive environmental conditions.

At the beginning of each campaign and every 24 hours after, we performed a zero calibration on the DX4040 using ultra-pure 99.999% N_2 gas. It is recommended that zero calibrations are performed every 24 hours and when the ambient temperature changes by 10°C, so the experiment was paused for ~30 minutes during the zero calibrations each day. Gas fluxes were calculated using Soil Flux Pro (v4.2.1, LICOR, Lincoln, Nebraska) and underwent standardized quality assurance and quality control protocol as established in previous publications (Capooci et al., 2019; Petrakis et al., 2017). QA/QC included several steps. First, all values due to instrumental errors such as an insufficient chamber closure seal were removed. These errors were identified by the SoilFluxPro software. Second, the R^2 for the linear and exponential fits of trace gas emissions were compared and the fit with the higher R^2 was chosen. Third, all fluxes that occurred when the R^2 of CO_2 was <0.90 were removed. Low R^2's indicate that the soil micrometeorological conditions were not stable during the measurement. Finally, all negative CO_2 fluxes were removed since they were likely erroneous.

2.4 Ancillary measurements

Meteorological (station: delsjmet-p) and water quality (station: Aspen Landing) data were obtained from the National Estuarine Research Reserve's Centralized Data Management Office (CDMO) and collected according to their protocol (System-wide Monitoring Program).

Meteorological data was collected using a CR1000 Meteorological Monitoring Station (Campbell Scientific, Logan, UT, USA). Water quality data were measured using a YSI 6600 sonde (YSI Inc., OH, USA). Both data sets were cleaned and gap-filled following the protocol established in Capooci et. al. (2022).

Phenological data were obtained from the PhenoCam network (site: stjones, Seyednasrollah et al., 2019) as described previously (Trifunovic et al., 2020; Hill et al., 2021). Briefly, a single mid-day photo (12:00:00 h) was selected for each of the days in the study period and was visually inspected to remove images with obvious distortions. Since the images included a variety of vegetation types, the region of interest delineated to only the area containing *S. alterniflora*, the main species at the study site. Then the phenopix R package (Filippa et al., 2020) was used to extract and calculate the greenness index, as well as delineate the phenophases for the study period (Hill et al., 2021).

2.5 Data analyses

Daily averages and associated standard deviations were calculated for meteorological and water quality data, except for the greenness index. Soil trace flux data were averaged into hourly and daily means and standard deviations. For heat maps, average hourly and campaign-length coefficients of variation were calculated.

We extracted measurements from the time series of the automated measurements to represent information collected from discrete temporal measurements conducted during daytime low tide. This approach aimed to represent a measurement protocol derived from manual (i.e., survey) measurements where most measurements are performed at daytime and low tide for logistical reasons. To identify and extract these measurements, we identified when low tide

occurred during each day (between 9:00:00 and 17:00:00 h) of the campaigns from water level data obtained from the tidal creek. All automated measurements that fell between 1 hour before and 1 hour after low tide were extracted, averaged into a daily value, and classified as "discrete" measurements. For example, if low tide fell at 13:00:00 h, all continuous measurements that fell between 12:00:00 and 14:00:00 h were then extracted and averaged to obtain a daily mean. Daily means were also calculated for all automated measurements collected during the day and will be referred to as the "continuous" daily mean. Differences in the means and distributions of the continuous and discrete fluxes were assessed using a t-test and a Kolmogorov-Smirnov test, respectively.

Sustained global warming potential (SGWP) was calculated for both the campaign-long and daytime low tide fluxes for CO_2, CH_4, and N_2O. SGWP accounts for sustained gas emissions over time compared to the global warming potential which accounts for a pulse emission over time (Neubauer and Megonigal, 2019). To calculate the SGWP, data from Day 2 and 3 of each campaign was used since measurements on Day 1 and 4 did not always occur during daytime low tide. Fluxes were converted into g m^{-2} and multiplied by the 20 and 100-year SGWP (Neubauer and Megonigal, 2019). SGWP were compared to see whether extrapolating SGWP from daily-averaged manual measurements done at low tide yielded similar values as hourly-averaged from high temporal frequency measurements.

3. Results

3.1 Meteorological and water quality

225 Air temperature and greenness index show traditional seasonal patterns of temperate salt
226 marshes (Fig. 1). Daily mean air temperature ranged from -3.5℃ to 29.9℃, with an average
227 daily temperature of 13.8 ± 9.1℃, while greenness index ranged from 0.30 to 0.42 with an
228 average of 0.34 ± 0.04. Relative humidity, barometric pressure, water level, and salinity varied
229 throughout the year. Relative humidity ranged from 32.6% to 100% with an average of 79.1% ±
230 16.7%. Barometric pressure was between 999.7 and 1036 mb with an average value of 1018.3 ±
231 6.8 mb. Daily water level ranged from -0.30 m to 0.76 m with an average height of 0.25 ± 0.2 m,
232 while salinity ranged from 1.1 ppt to 20.4 ppt with an average of 8.0 ± 4.45 ppt.
233

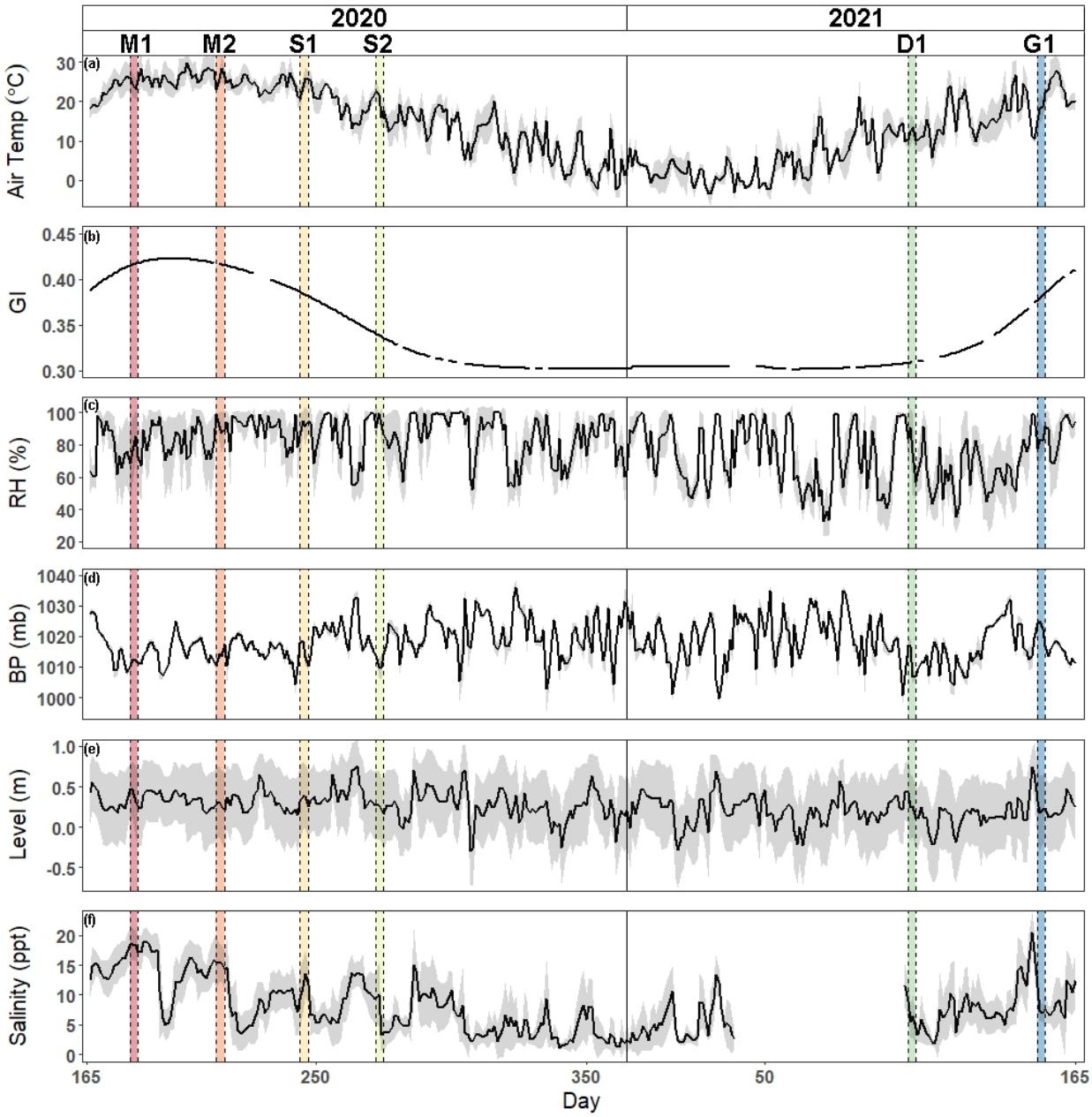

234

235 **Figure 1.** Time series of hourly mean ± SD (gray shaded region of (a) air temperature, (b)

236 greenness index, (c) relative humidity, (d) barometric pressure, (e) water level, and (f) salinity

237 from June 14, 2020 to June 14, 2021. Vertical shaded areas correspond to each of the campaigns

238 (M = maturity, S = senescence, D = dormancy, G = greenup).

239

240

241 *3.2 Greenhouse gas and sulfur-based trace gas patterns and variability*

242 Average CO_2 fluxes were significantly different in each campaign, with the highest
243 average fluxes occurring during the G1 campaign and the lowest during the D1 campaign (Fig.
244 2a). During some campaigns, such as S1, CO_2 fluxes did not show similar temporal patterns
245 between chambers, whereas during other campaigns, such as M2 and G1, all six chambers had
246 similar patterns. While there is a seasonal pattern in CO_2 fluxes, with higher fluxes occurring
247 during warmer months, diel patterns were not consistent between campaigns. One notable
248 exception is the G1 campaign, during which a clear diel pattern was observed. CO_2 fluxes had
249 consistent variability from one hour to the next during each of the 6 campaigns (Fig. 3a), with
250 overall average variability ranging from 28.9% during M2 to 49.6% during Dl.

251 CH_4 fluxes were low most of the time, particularly during the G1 campaign (Fig. 2b).
252 However, CH_4 pulses occurred during 5 out of the 6 campaigns, with S1and S2 having the most
253 frequent pulse emissions. S2 had the largest CH_4 pulse,13,488 nmol m^{-2} s^{-1}, which was 2,599%
254 higher than the average flux. The highest average CH_4 fluxes also occurred during S1 and S2,
255 while the highest hourly variability occurred in both S1 and S2, as well as in M2 (Fig. 3b). Mean
256 CH_4 variability ranged from -108% in M1 to 91.0% in S1.

257 Most N_2O fluxes were near-zero, with periodic pulses of emissions or uptake that ranged
258 from -33.8 to 19.0 nmol m^{-2} s^{-1} (Fig. 2c), with a maximum percent change from the mean of
259 10,231%. Four out of the six campaigns (M1, S2, D1, and G1) had net N_2O uptake, while two
260 campaigns (M2, S1) had net N_2O fluxes. There were no significant differences between
261 campaigns except for M1 and S1. Meanwhile, N_2O fluxes had very high hourly variability
262 ranging from -106,964% to 26,208% (Fig. 3c). Consequently, average variability during each
263 campaign was highly variable from -1,032% to 129%.

Similarly to CH_4 and N_2O, CS_2 fluxes were low the majority of the time, with occasional pulses of emissions or uptake (Fig. 2d). CS_2 fluxes ranged from -386.9 to 306.2 nmol m^{-2} s^{-1}, with a maximum percent change from the mean of 4,785%. All campaigns had net emissions despite periodic pulses of CS_2 uptake. CS_2 fluxes also had high hourly variability, with overall means for each campaign ranging from -70.2% during D1 to 2254% during M2 (Fig. 3d).

DMS emissions were zero for most of the campaigns (Fig. 2e). Pulses of emissions and uptake tended to occur during mid-day. DMS fluxes ranged from -158.5 to 230 nmol m^{-2} s^{-1}, with a maximum percent change from the mean of 185,987%. D1 and G1 had net uptake, while the other four campaigns had net emissions of DMS. During periods of emissions and uptake, hourly variability ranged from -870.5% to 888.7% (Fig. 2e). The extended periods of no DMS fluxes contributed to low overall mean variability during each campaign, ranging from -2.45% in S2 to 35.7% in M2.

277

278 **Figure 2.** Time series of fluxes from each chamber during each campaign for (a) CO_2, (b) CH_4,

279 (c) N_2O, (d) CS_2, and (e) DMS. Each color designates a different chamber. The campaign means

280 [LCI = lower 95% confidence interval, UCI = upper 95% confidence interval] are listed on each

281 panel. The y-axis for CH_4 fluxes was shortened to show the variability. Full range of CH_4 fluxes

282 during S2 can be seen in Supplementary Figure (SF) 1.

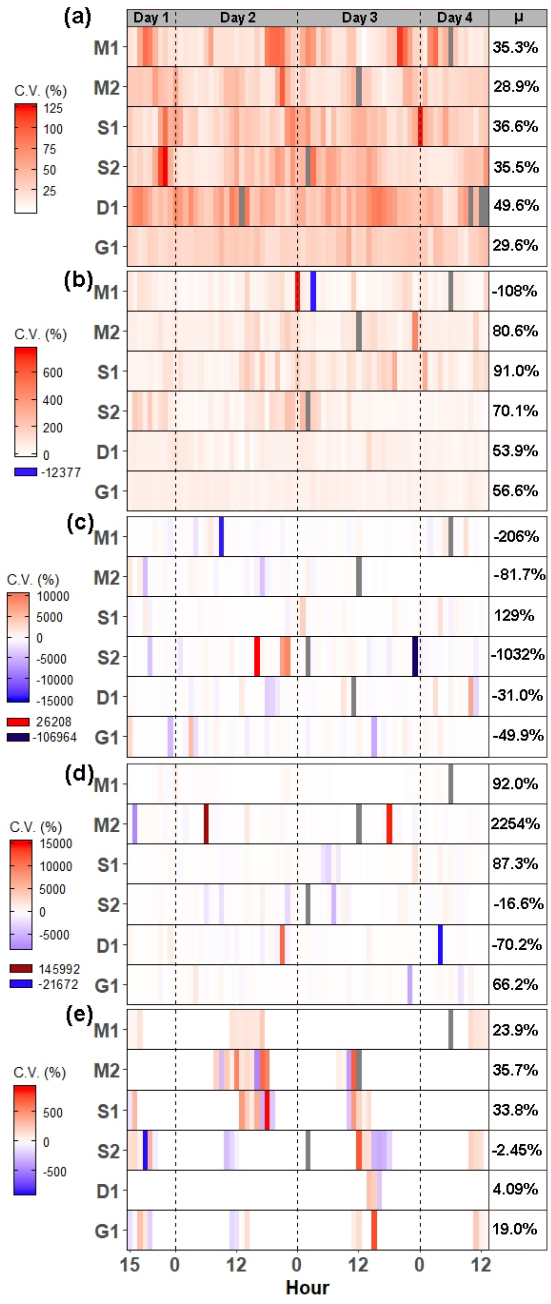

283

284 **Figure 3.** Heat maps of hourly coefficient of variance (CV) for (a) CO_2, (b) CH_4, (c) N_2O, (d)

285 CS_2, and (e) DMS during each campaign. Each pixel represents the average CV for that hour.

286 Mean CV for each campaign is listed in the μ column. Grayed out pixels represent NA. Note:

287 legend scale is different for each gas and campaigns start at 15:00:00 h on Day 1 and end at

288 13:00:00 h on Day 4.

289 *3.3 Comparisons between continuous and discrete measurement scenarios*

290 A subset of the continuous measurements that fall during daytime low tide was selected
291 to represent data collected using traditional discrete, manual measurements which are commonly
292 reported for tidal salt marshes. Information from continuous and discrete datasets are compared
293 to elevate whether they provide similar distributions, daily means, flux-temperature
294 relationships, and SGWP.

295 Continuous and discrete flux distributions can be seen via density plots (Fig. 4). While
296 the distributions for continuous and discrete fluxes overlap for each of the five gases, four of the
297 five gases have significantly different distributions of fluxes when comparing the continuous and
298 the discrete datasets (Table 1). The only gas that had similar distributions between the two
299 sampling intervals was CO_2 (Table 1). For all gases, the continuous distribution had higher
300 kurtosis values and higher C.V. than the discrete fluxes (Table 1). Of the five gases, CS_2 was the
301 only one with a more skewed discrete data distribution and significantly different means between
302 continuous and discrete measurement scenarios (Fig. 4b, Table 1).

303 For CS_2 and DMS, discrete measurements had higher overall daily mean fluxes (Fig. 5d,
304 5e), while the opposite occurred for CH_4 and N_2O (Fig. 5b, 5c). CO_2 fluxes from continuous and
305 discrete measurements had nearly a 1:1 relationship (Fig. 5a). Both CO_2 and DMS had strong
306 relationships between continuous and discrete daily means, with r-squares higher than 0.7, while
307 N_2O and CS_2 had moderate relationships. CH_4 had a poor fit between continuous and discrete
308 measurements.

309 Next, relationships between trace gas flux and air temperature were evaluated for each
310 gas under continuous and discrete measurement scenarios. CO_2 and CH_4 fluxes had statistically
311 significant relationships for both discrete and continuous measurements versus air temperature

312 (Fig. 6a-d). Air temperature explained 38% and 21% of the variability for discrete and
313 continuous measurements for CO_2, respectively (Fig. 6a, b), while air temperature explained
314 32% and 7% of the variability for discrete and continuous measurement for CH_4 (Figs. 6c, d).
315 The slopes for both discrete and continuous CO_2 fluxes were not significantly different (95% CI;
316 0.029 - 0.12, 0.037 - 0.054, respectively), as well as for CH_4 (95% CI; 2.14 - 12.7, 1.31 - 2.71,
317 respectively). For N_2O, CS_2, and DMS, there were no significant relationships between discrete
318 daily mean fluxes and air temperature, but there were significant relationships between
319 continuous hourly mean fluxes and air temperature (Fig. 6e-j). Air temperature explained very
320 little variability for N_2O, CS_2, and DMS.
321 Discrete measurements had a higher SGWP potential than the continuous measurements
322 (Table 2). While the discrete measurements had a slightly lower SGWP for CO_2 and a slightly
323 higher SWGP for N_2O, the difference between continuous and discrete SGWP was driven by
324 CH_4. The 20-yr and 100-yr SGWP for discrete measurements of CH_4 were up to ~38% higher
325 than the respective continuous measurements, contributing to an overall increase of ~18% and
326 ~11% for the discrete measurement's 20- and 100-year SGWP.
327

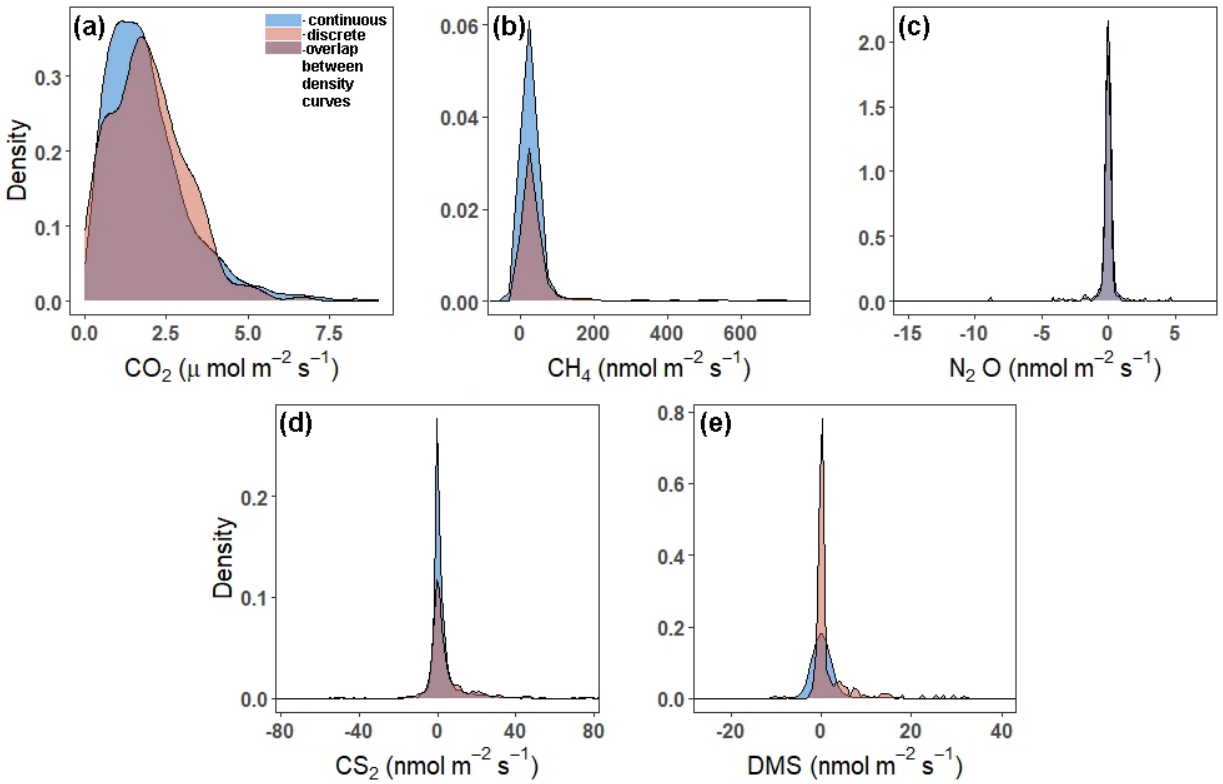

328

329 **Figure 4.** Density plots comparing the distribution of fluxes throughout all campaigns

330 (continuous over ~72 hours) to those measured during daytime low tide (discrete, one hour

331 before and one hour after daytime low tide) for (a) CO_2, (b) CH_4, (c) N_2O, (d) CS_2, and (e) DMS.

332 Note: The scales on the x- and y-axes are different. The tails have been cut off to better see the

333 peaks for (b), (c), (d), and (e). To see plots with full distributions, see SF 2.

Table 1. Summary of continuous (over ~72 hours) and discrete (one hour before and one hour after low tide) measurement data and distributions for each gas. An alpha of < 0.05 was used to determine significant differences between the means and the distributions. Note: Means for CO_2 are in μmol m^{-2} s^{-1}, while the other gases are in nmol m^{-2} s^{-1}.

Gas	Sampling Frequency	Mean	95% CI	C.V.	Skewness	Kurtosis	Means Different?	Distributions Different?
CO_2	Continuous	1.92	1.86–1.97	67.2%	1.53	6.51	No	No
	Discrete	1.90	1.74–2.07	62.3%	0.67	3.65		
CH_4	Continuous	41.2	29.5–52.9	708%	41.6	1903	No	Yes p = 0.02
	Discrete	57.6	39.2–76.0	234%	5.21	34		
N_2O	Continuous	-0.06	-0.13–0.009	2686%	-4.67	133	No	Yes p < 0.001
	Discrete	-0.16	-0.29–-0.04	556%	-4.39	47.8		
CS_2	Continuous	3.39	2.45–4.33	673%	1.51	116	Yes p = 0.04	Yes p = 0.05
	Discrete	6.44	3.70–9.18	312%	3.93	22.9		
DMS	Continuous	1.11	0.70–1.51	907%	8.74	223	No	Yes p < 0.001
	Discrete	1.77	1.06–2.48	295%	3.40	16.6		

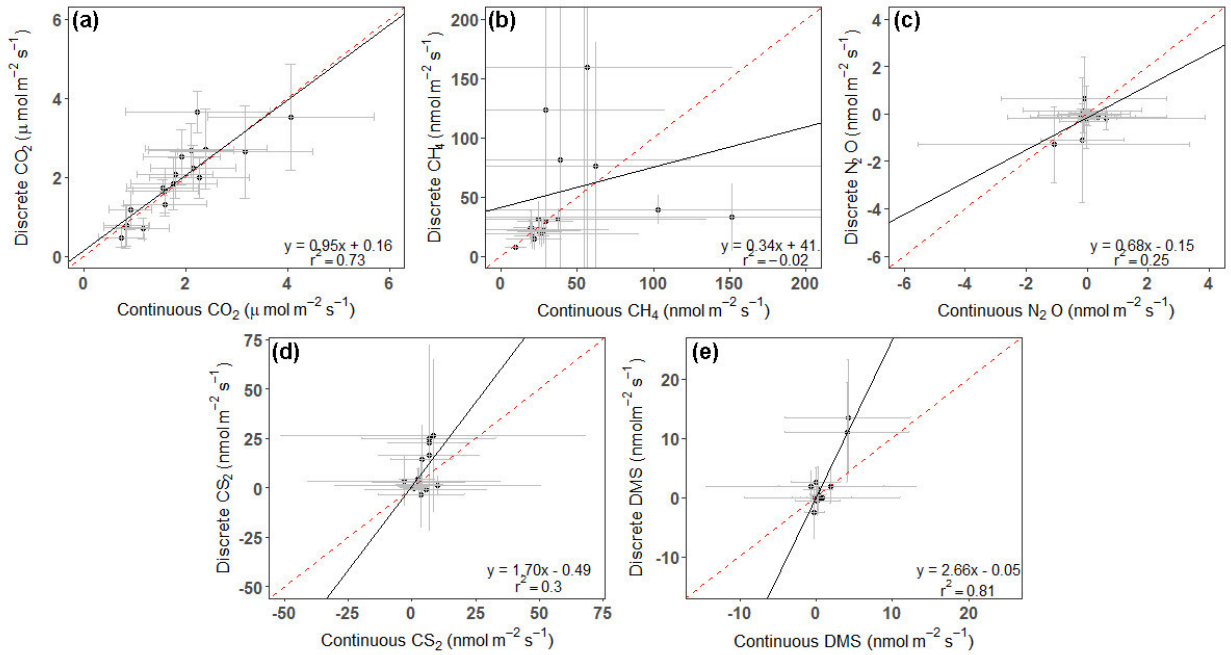

340

341

342 **Figure 5.** Plots comparing the daily average of continuous (over ~72 hours) to discrete (one hour
343 before and one hour after daytime low tide) measurements for (a) CO_2, (b) CH_4, (c) N_2O, (d)
344 CS_2, and (e) DMS. Error bars represent the SD and have been cut off in panel (b) to show data
345 better. See SF 3 for full error bars for panel b. Red dashed line is the 1:1 line, while the black
346 solid line is the trend line.

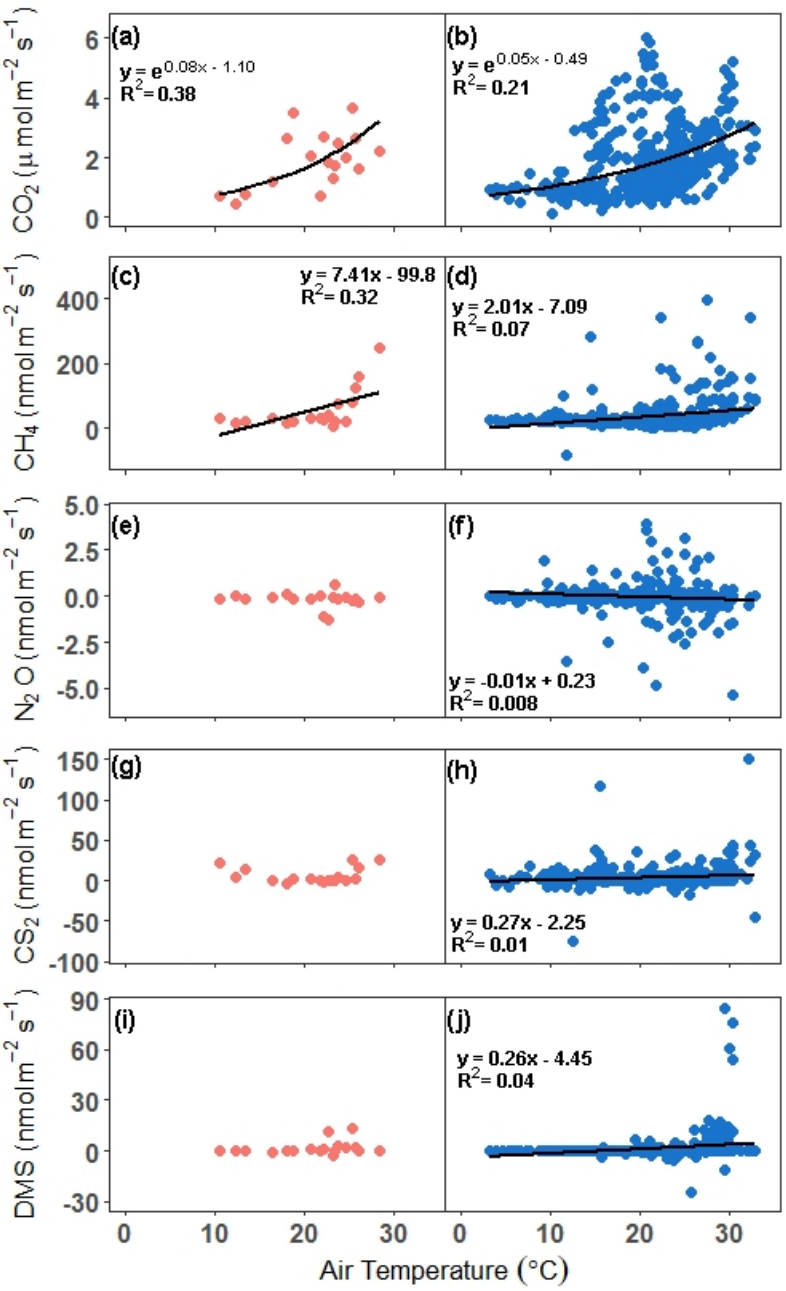

347

348 **Figure 6.** Comparison of fluxes versus air temperature for all campaigns. In panels, a, c, e, g, and

349 I, the hourly continuous (over ~72 hours) mean is compared to the hourly air temperature, while

350 in panels b, d, f, h, and k, the discrete (one hour before and one hour after daytime low tide) daily

351 mean is compared to the daily air temperature. The trend lines for significant relationships at

alpha <0.05 are plotted. Note: In panel d, the outlier hourly mean of 2,275 nmol m^{-2} s^{-1} is not included in the trend line or in the graph.

Table 2. Sustained global warming potential (SGWP) derived from continuous (over ~72 hours) and discrete (one hour before and one hour after daytime low tide) temporal measurements in a tidal salt marsh.

Frequency	CO_2 (g m^{-2})	CH_4 ($CO_{2\text{-eq}}$ (g m^{-2}))		N_2O ($CO_{2\text{-eq}}$ (g m^{-2}))		Total ($CO_{2\text{-eq}}$ (g m^{-2}))	
		20-yr SGWP	100-yr SGWP	20-yr SGWP	100-yr SGWP	20-yr SGWP	100-yr SGWP
Continuous	84.9	70.4	33.0	0.27	0.30	155.57	118.2
Discrete	82.7	103.2	48.4	0.40	0.44	186.3	131.54

4. Discussion

4.1 Measuring all the time: seasonal and diel patterns and hot moments of soil trace gases

Spatial variability between the individual chambers at SS were low, but CO_2 fluxes showed temporal variability that corresponded to changes in temperature. The relatively low spatial variability within our experimental setting contrasts with previously reported high spatial variability of CO_2 fluxes attributed to the presence of a hot spot (Capooci and Vargas, 2022). However, previous CO_2 fluxes measured at the SS site ranged from 0-15 μmol m^{-2} s^{-1}, with the bulk of the measurements between 0-5 μmol m^{-2} s^{-1}, with higher fluxes associated with hot spots or warmer temperatures (Capooci and Vargas, 2022; Seyfferth et al., 2020; Hill and Vargas, 2022). Therefore, location of measurements within a landscape could be influenced by hot spots,

371 which complicates ecosystem scale calculations of soil CO_2 fluxes (Barba et al., 2018). In
372 addition, there was a seasonal pattern evident in the CO_2 fluxes, with higher emissions during the
373 growing season, as typical in temperate ecosystems, as well in the significant relationship
374 between CO_2 and air temperature. Within salt marshes, soil organic matter decomposition into
375 products such as CO_2 correlates with temperature due to the activation energy needed for organic
376 matter breakdown (McTigue et al., 2021). Other studies at temperate wetland sites have found
377 higher fluxes during the summer (Simpson et al., 2019; Yu et al., 2019; Bridgham and
378 Richardson, 1992), as well as relationships between CO_2 fluxes and temperature (Capooci and
379 Vargas, 2022; Simpson et al., 2019; Xie et al., 2014) highlighting that CO_2 fluxes in temperate
380 salt marshes exhibit a temperature dependency over seasonal scales, even in the presence of
381 tides.

382 While CO_2 fluxes show seasonal patterns, there are no diel patterns that persist
383 throughout the year. During G1, the peak of high tide coincided with peak daily temperature.
384 This scenario also occurred during D1, but fluxes were too low to discern patterns. During all
385 other campaigns, low tide and peak temperatures coincided. These results suggest that diel
386 patterns may occur periodically under certain conditions. For example, at the SS site, it may be
387 that diel patterns occur during high tide at the temperature peak. While we expected the highest
388 fluxes during low tides due to increased oxygen exposure, there may be a lag between low tide in
389 the creek and low water levels at the SS site, resulting in higher fluxes during high tide in the
390 creek. However, these results can vary from site to site and with proximity to the tidal creek.
391 More research using high temporal frequency measurements are needed to parse out the role of
392 temperature and tides on CO_2 fluxes across salt marshes to properly represent the pattern in earth
393 system models (Ward et al., 2020)

Similarly to CO_2, CH_4 has a significant relationship with air temperature, however it explains less variability in the fluxes. Several studies have found positive correlations between soil CH_4 fluxes and temperature (Bartlett et al., 1985; Emery and Fulweiler, 2014; Wang and Wang, 2017) in temperate salt marshes, while others have not (Wilson et al., 2015). It is important to note that while, in general, salt marsh CH_4 fluxes are positively related to temperature (Al-Haj and Fulweiler, 2020), the ability of temperature to explain CH_4 flux variability is low, compounded by many, often site-specific, factors that affect methane production and consumption, such as organic matter supply, microbial communities, and diffusion rates (Al-Haj and Fulweiler, 2020; Bartlett et al., 1985).

At our study site, CH_4 fluxes were highest and pulses were most frequent during senescence, agreeing with findings from ecosystem-scale measurements derived using the eddy covariance technique (Vázquez-Lule and Vargas, 2021). In most wetland ecosystems, including those in northern, temperate, and subtropical areas, the highest fluxes have been reported during the summer (Kim et al., 1998; Rinne et al., 2007; Van Der Nat and Middelburg, 2000; Livesley and Andrusiak, 2012; Turetsky et al., 2014), but we highlight that there is a lack of measurements during the winter (Al-Haj and Fulweiler, 2020). In *S. alterniflora* marshes, highest mean CH_4 fluxes have been found in both the summer and the fall (Bartlett et al., 1985; Emery and Fulweiler, 2014). At a site dominated by *S. alterniflora,* both high fluxes and porewater CH_4 concentrations were found in September (Zhang and Ding, 2011), indicating either a continual build-up of CH_4 in the porewater over the growing season and/or increased CH_4 production in the fall. For our site, it is likely higher CH_4 emissions during senescence were due to an input of labile organic matter from plant die-off (Seyfferth et al., 2020). Furthermore, a recent study has shown that porewater DMS, a non-competitive substrate for methylotrophic methanogenesis that

417 is produced from the breakdown of DMSP, a metabolite produced by *S. alterniflora* (Dacey et
418 al., 1987), peaks during the fall (Tong et al., 2018). Therefore, we postulate that an influx of
419 DMS may also contribute to higher CH_4 fluxes during senescence in marshes dominated by *S.*
420 *alterniflora*. This finding highlights the importance of carbon-sulfur biogeochemistry and
421 measuring fluxes during non-summer months; particularly in marshes that have plant
422 communities that provide substrates used in methylotrophic methanogenesis (Seyfferth et al.,
423 2020).

424 On a diel timescale, pulse emissions of CH_4 from the soil tend to occur during the
425 warmest time of the day, as well as during low and rising tides. There are very few studies that
426 report high-temporal frequency data of CH_4 emissions, most of which include plants within their
427 scope (via transparent chambers or eddy covariance) or focus on tidal creeks, making it difficult
428 to ascertain whether the diel patterns seen in this study are typical of tidal salt marsh soils. Of the
429 studies that report high-temporal frequency data of plant or water-based CH_4 fluxes in coastal
430 vegetated ecosystems, CH_4 emissions have been found to peak at various points in the day, from
431 during the day (Yang et al., 2018, 2017; Tong et al., 2013), at night (Diefenderfer et al., 2018), or
432 highly variable (Jha et al., 2014; Xu et al., 2017). At our site, CH_4 fluxes tended to peak at the
433 confluence of peak daily temperature and low to rising tides, indicating that physical forcing may
434 contribute to CH_4 pulses (Bahlmann et al., 2015; Middelburg et al., 1996). However, pulses did
435 occur during other times throughout the day and within the tidal cycle. While some of the pulse
436 emissions may be a result of ebullition, the majority are associated with high R^2's, indicating that
437 they are sustained over the measurement period. Our results demonstrate the importance of
438 conducting high-temporal frequency CH_4 measurements in tidal salt marsh soils for several

reasons, including the need for more data to better understand the drivers of CH_4 fluxes at diel scales and how that affects model predictions.

N_2O emissions and uptake loosely followed a seasonal pattern, likely driven by the canopy phenological stages. During the growing season, it has been shown that highly productive plants can compete with soil microbes for NO_3^- and NH_4^- (Cheng et al., 2007; Yu et al., 2012; Zhang et al., 2013; Granville et al., 2021; Xu et al., 2017), shifting denitrifiers into consuming N_2O and resulting in a net uptake during G1 and M1. As the plants reach peak maturity, the system shifts into net emission of N_2O during M2 and S1. One study found that nitrogen additions resulted in a pulse of N_2O in July when most of the plant growth had occurred, but no response in April, suggesting that the competition for NO_3^- and NH_3^+ decreases when plant growth has slowed down (Moseman-Valtierra et al., 2011). Increased substrate availability combined with warm temperatures likely contributed to the marsh being a net source of N_2O during the later stages of the growing season. As temperatures drop, the system shifts back into net uptake, as seen during S2 and D1. Similar seasonal patterns have been seen in other studies, albeit shifted by a month or two depending on the local climate and phenophases (Granville et al., 2021; Emery and Fulweiler, 2014). These findings highlight balance between processes that produce N_2O (e.g., nitrification, denitrification, and nitrifier-denitrification) and consume N_2O (e.g., denitrification), as well as substrate availability and plant phenology in determining whether a marsh is a source or sink of N_2O at any given point.

As with seasonality, diel patterns of N_2O showed both emissions and uptake. Several studies have also reported both emissions and uptake during a 24-hour period (Yang et al., 2017; Tong et al., 2013). We found that pulses of uptake and emissions occurred both during the day and at night, as well as during different phases of the tidal cycle. Studies have found higher

462 fluxes during the day (Tong et al., 2013; Yang et al., 2017) and at night (Laursen and Seitzinger,
463 2002; Yang et al., 2017; Bauza et al., 2002). Generally, fluxes were slightly higher at night
464 throughout the campaigns, perhaps as a result of increased availability of NH_4^+ at night due
465 decreased competition from photosynthesizers (Bauza et al., 2002). Overall, N_2O fluxes were
466 near-zero with a < 0.50 nmol m^{-2} s^{-1} difference between daytime and nighttime mean fluxes,
467 suggesting that N_2O fluxes do not play a major role in GHG emissions at this salt marsh.
468 Our automated measurements of sulfur-based trace gases show high variability in CS_2,
469 with low fluxes punctuated by occasional pulse emissions. There are no previous studies with
470 automated measurements to compare our findings, but previous studies have noted that CS_2
471 fluxes are highly variable (Steudler and Peterson, 1985; Hines, 1996), with periods of emission
472 and uptake. However, fluxes at SS were, on average, an order of magnitude higher than values
473 reported in the literature (Supplementary Table 1). There could be several reasons for the
474 difference in magnitudes: 1) improvement in instrumentation to detect CS_2, 2.) sampling
475 technique differences, and 3.) site-specific characteristics. Since the influx of sulfur-based trace
476 gas measurements in the 1980s, instrumentation has advanced from using molecular sieves and
477 cryotraps to store samples before measuring them on a gas chromatograph (e.g., Carroll et al.,
478 1986; Cooper et al., 1987; Steudler and Peterson, 1984) to using portable Fourier transform
479 infrared (FTIR) spectrometers that measure trace gas concentrations in near real-time. These
480 instrumentation advances subsequently led to changes in sampling techniques. Traditionally, it
481 was common to keep the chamber closed for upwards of 24-hours, with samples being collected
482 over hourly intervals throughout the day (Carroll et al., 1986; Goldan et al., 1987). Sweep air
483 free of sulfur trace gases was also commonly used to avoid the need to take samples at both the
484 inlet and outlets of the chambers (Goldan et al., 1987). However, others used ambient air because

485 it more closely resembled *in situ* conditions (Steudler and Peterson, 1985). With recent advances,
486 sampling techniques have changed to eliminate the need for very long closure times and reduce
487 the effects the chambers have on micrometeorological conditions. Now, high-temporal
488 frequency, long-term data can be obtained, thereby capturing pulse emissions that otherwise may
489 be missed. The third reason for difference in magnitude could be due to site-specific differences
490 in CS_2 fluxes. While the mechanisms by which CS_2 is produced are poorly understood, there are
491 several potential production pathways: OM degradation, photochemical production, and algal
492 production (Xie and Moore, 1999). The most likely pathway for our site is the microbially-
493 mediated reaction between H_2S and organic matter due to high sulfur concentrations, anaerobic
494 conditions, and a large pool of decaying organic matter. Finally, CS_2 is a short-lived sulfur gas
495 but the major product of CS_2 oxidation is COS; consequently, understanding CS_2 production and
496 oxidation is important for recognizing the role of salt marshes in COS dynamics (Whelan et al.,
497 2013).

498 The mean of measured DMS fluxes generally fall within those reported in the literature,
499 but with pulses higher than previously reported and different temporal patterns. We found that
500 DMS fluxes only occurred during the middle of the day, near when air temperatures peaked. This
501 is contrary to several studies that have found DMS fluxes during other times of the day
502 (Morrison and Hines, 1990; Steudler and Peterson, 1985; DeLaune et al., 2002). Some studies
503 have found diel patterns related to temperature (De Mello et al., 1987; Cooper et al., 1987b) and
504 incoming tides (Morrison and Hines, 1990; Dacey et al., 1987; Goldan et al., 1987). Our results
505 indicate that DMS fluxes from the SS site are associated with temperature and light-related
506 processes, whether these variables influence microbial activity, plant physiology, or a
507 combination of both. A study found that DMS fluxes peaked after a full daylight period in a

508 Danish estuary (Jørgensen and Okholm-Hansen, 1985). However, there is no information on the
509 diel patterns of DMS in the sediment pore water or its release from *S. alterniflora* plants. DMS is
510 also produced by other pathways that occur under anoxic conditions, such as methylation of
511 sulfide and methanethiol (Lomans et al., 2002; Sela-Adler et al., 2015), microbial reduction of
512 dimethylsulfoxide (Capone and Kiene, 1988), and/or the incorporation of inorganic substrates
513 (i.e., CO_2) and organic methylated compounds (Finster et al., 1990; Moran et al., 2008; Lin et al.,
514 2010). To better understand DMS fluxes, more research into the dynamics between *S.*
515 *alterniflora*, pore water DMS, and DMS fluxes is needed, as it plays an important role in carbon-
516 sulfur biogeochemistry, particularly as a non-competitive substrate for methylotrophic
517 methanogenesis (Seyfferth et al., 2020) .
518
519 *4.2 Continuous versus discrete measurements: do we get the same information?*
520 Our results show that discrete temporal measurements of CO_2 during daytime low tide
521 throughout the year (including dormancy) may be sufficient to obtain a representative mean of
522 the temporal variability of soil CO_2 flux. This has implications for calculating carbon budgets.
523 Furthermore, the distribution of continuous and discrete CO_2 fluxes is similar, indicating that
524 discrete measurements are capturing similar variability as continuous measurements. This
525 observation is reinforced by the CO_2 ~ air temperature relationships, which do not have
526 significantly different slopes (discrete: 0.03 - 0.12, continuous: 0.04 - 0.05), providing further
527 support for the utility of daytime low tide discrete measurements in evaluating potential drivers
528 of CO_2 variability.
529 In contrast, high variability in CH_4 fluxes resulted in the means for discrete and
530 continuous measurements to be similar, but with significantly different distributions. In salt

marshes, CH_4 fluxes are characterized by high variability (Rosentreter et al., 2021), making it difficult to assess the processes that control CH_4 fluxes (Vázquez-Lule and Vargas, 2021). While the means were not significantly different despite ~33% higher mean flux using discrete measurements, it is important to note that the 95% confidence interval and the coefficient of variation are broad and very high, resulting in potential error cancellation for the calculation of the mean. We postulate that the discrete measurement approach can be used to calculate budgets with the caveat of large uncertainties and that they likely overestimate the mean CH_4 flux. Discrete measurements do not capture similar variability as the continuous measurements and have a stronger air temperature-CH_4 flux relationship than continuous measurements, despite the overlap between their confidence intervals (2.14 - 12.7 and 1.31 - 2.71, respectively). However, continuous measurements provide a more accurate depiction of the patterns and magnitudes of CH_4 and can provide stronger insights into the interrelated drivers of CH_4 fluxes.

Regardless of the sampling interval, N_2O fluxes had means that are near-zero. Due to fluxes consistently being near zero, the discrete and continuous measurements will likely get similar overall results due to error cancellation even if the distributions were significantly different. The continuous measurements capture a wider range of fluxes than the discrete measurements, as seen with its very high coefficient of variance and a different distribution. However, the skewness between the two approaches is very similar, due to the bulk of the measurements falling around the same values as seen in the large amount of overlap in the density curves. It is important to note that this site is nitrogen-limited, which constrains N_2O production. In marshes that are not nitrogen-limited, sampling intervals will likely play a more important role since fluxes will be higher.

For CS_2, discrete and continuous measurements did not have similar means or distributions, likely due to the high variability found in these measurements. Previous studies using discrete measurements of CS_2 have noted its high variability (e.g. De Mello et al., 1987), with one highlighting the need for frequent measurements of sulfur-based trace gases during the day in order to obtain an accurate mean daily flux value (Steudler and Peterson, 1985). We found that discrete measurements taken during daytime low tide result in a daily mean that is nearly twice that of the daily mean from the continuous measurements. The average CS_2 fluxes measured during our field campaigns were up to an order of magnitude higher than previously reported. We advocate for more measurements of CS_2 fluxes beyond focusing on low tide windows and during different canopy phenological phases across salt marshes to better understand the dynamics of this trace gas.

When measuring DMS fluxes during daytime low tide, the mean is similar to the continuous measurement mean, but the distributions are significantly different. However, caution should be taken in using discrete measurements of DMS to calculate daily means, particularly if those measurements fall during the warmest part of the day when DMS fluxes are the most active. This could result in overestimating the daily mean since extended periods of no fluxes are not accounted for. One approach to measuring DMS fluxes would be to use the strong relationship between discrete and continuous measurements to correct for the overestimation of discrete fluxes. However, this approach would still require the use of a continuous, automated system at different points throughout the year to establish a site-specific correction of discrete mean DMS fluxes, particularly if DMS fluxes are used to calculate DMS budgets.

5. Conclusion: what are we missing and challenges

576 Discrete measurements have the clear advantage of capturing the spatial variability of soil
577 trace gas fluxes across an ecosystem, but this approach is also used to describe the temporal
578 variability. In contrast, continuous measurements using autochambers accurately describe
579 temporal patters (e.g., hourly measurements) but have limited spatial representation due to high
580 instrumentation costs and limited spatial extent of the area where autochambers can be deployed
581 (Vargas et al., 2011; Barba et al., 2018). Here we discuss the advantages and differences from
582 discrete and continuous measurements derived from this study.
583 Discrete measurement campaigns are suitable for calculating budgets, particularly for
584 CO_2 and N_2O since they capture comparable means, but not the temporal variability nor
585 functional relationships (e.g., temperature dependency) as continuous measurements. While we
586 found that CH_4 and DMS means were not significantly different between the two approaches,
587 there are caveats that must be considered when using discrete measurements. The high variability
588 inherent in CH_4 fluxes can contribute to the lack of significant differences between the two
589 approaches and result in discrete measurements overestimating the overall CH_4 fluxes from a
590 tidal salt marsh. This has implications when calculating SWGP where differences in CH_4 means
591 largely contribute to the differences in SGWP between the two approaches and can affect how
592 scientists and policymakers view tidal salt marshes and blue carbon as a natural climate solution
593 (Macreadie et al., 2021). For DMS, it is important to assess diel patterns to ensure that fluxes are
594 representative, particularly at sites that have patterns similar to what is seen at our study site.
595 When evaluating variability or trying to parse out the processes that drive GHG and trace
596 gas emissions from tidal salt marshes (e.g., functional relationships), using continuous,
597 automated measurements would be the best approach. This is particularly important for CH_4,
598 where pulse emissions are frequent during the growing season and can be very high. Using

continuous measurements is also important in scenarios where discrete measurements do not capture a similar mean or distribution, as with CS_2 fluxes. We recognize that continuous measurements are expensive and difficult to implement across study sties, but we advocate for revisiting monitoring protocols and identifying potential biased interpretation of trace gas flux information from discrete measurements. Discrete measurements are more capable of representing spatial variability, and until we have a better understanding of which source of variability is higher, temporal or spatial, both techniques should be considered for ecosystem assessments.

Data availability

Meteorological (station: delsjmet-p) and water quality (station: Aspen Landing) data are available from the National Estuarine Research Reserve's Centralized Data Management Office (CDMO) at https://cdmo.baruch.sc.edu/. Phenological data are available from the PhenoCam network (site: stjones) at https://phenocam.sr.unh.edu/webcam/sites/stjones/. Data from trace gas fluxes are available in Figshare (doi:10.6084/m9.figshare.20449131).

Author contributions

MC and RV conceptualized the study, designed the methodology, and conducted project administration. MC conducted the formal analysis, investigation, and visualization, as well as wrote the original draft. RV provide funding, resources, supervision, as well as reviewed and edited the manuscript.

Competing interests

The authors declare that they have no conflict of interest.

Acknowledgments

This research was supported by the National Science Foundation (#1652594). MC acknowledges support from an NSF Graduate Research Fellowship (#1247394). We thank the onsite support from Kari St. Laurent and the Delaware National Estuarine Research Reserve (DNERR), as well as from Victor and Evelyn Capooci for field assistance during the first campaign. We thank George Luther for inspiring discussions about carbon-sulfur biogeochemistry in salt marshes. The authors acknowledge the land on which they conducted this study is the traditional home of the Lenni-Lenape tribal nation (Delaware nation).

References

Al-Haj, A. N. and Fulweiler, R. W.: A synthesis of methane emissions from shallow vegetated coastal ecosystems, Glob. Chang. Biol., 26, 2988–3005, https://doi.org/10.1111/gcb.15046, 2020.

Andreae, M. O. and Jaeschke, W. A.: Exchange of sulfur between biosphere and atmosphere over temperate and tropical regions, in: Sulfur Cycling on the Continents, edited by: Howarth, R. W., Stewart, J. W. B., and Ivanov, M. V., Wiley, New York, 1992.

Bahlmann, E., Weinberg, I., Lavrič, J. V, Eckhardt, T., Michaelis, W., Santos, R., and Seifert, R.: Tidal controls on trace gas dynamics in a seagrass meadow of the Ria Formosa lagoon (southern Portugal), 12, 1683–1696, https://doi.org/10.5194/bg-12-1683-2015, 2015.

Barba, J., Cueva, A., Bahn, M., Barron-Gafford, G. A., Bond-Lamberty, B., Hanson, P. J., Jaimes, A., Kulmala, L., Pumpanen, J., Scott, R. L., Wohlfahrt, G., and Vargas, R.: Comparing ecosystem and soil respiration: Review and key challenges of tower-based and soil measurements, Agric. For. Meteorol., 249, 434–443, https://doi.org/10.1016/j.agrformet.2017.10.028, 2018.

Barbier, E., Hacker, S., Kennedy, C., Stier, A., and Silliman, B.: The value of estuarine and coastal ecosystem services, Ecol. Monogr., 81, 169–193, 2011.

Bartlett, K. B., Harriss, R. C., and Sebacher, D. I.: Methane Flux from Coastal Salt Marshes, J. Geophys. Res., 90, 5710–5720, 1985.

Bauza, J. F., Morell, J. M., and Corredor, J. E.: Biogeochemistry of nitrous oxide production in the red mangrove (Rhizophora mangle) forest sediments, Estuar. Coast. Shelf Sci., 55, 697–704, https://doi.org/10.1006/ecss.2001.0913, 2002.

Bridgham, S. D. and Richardson, C. J.: Mechanisms controlling soil respiration (CO2 and CH4) in southern peatlands, Soil Biol. Biochem., 24, 1089–1099, https://doi.org/10.1016/0038-0717(92)90058-6, 1992.

Brühl, C., Lelieveld, J., Crutzen, P. J., and Tost, H.: The role of carbonyl sulphide as a source of stratospheric sulphate aerosol and its impact on climate, Atmos. Chem. Phys., 12, 1239–1253, https://doi.org/10.5194/acp-12-1239-2012, 2012.

Capone, D. G. and Kiene, R. P.: Comparison of microbial dynamics in marine and freshwater sediment, Limnol. Ocean., 33, 725–749, 1988.

Capooci, M. and Vargas, R.: Diel and seasonal patterns of soil CO2 efflux in a temperate tidal marsh, Sci. Total Environ., 802, https://doi.org/10.1016/j.scitotenv.2021.149715, 2022.

Capooci, M., Barba, J., Seyfferth, A. L., and Vargas, R.: Experimental influence of storm-surge salinity on soil greenhouse gas emissions from a tidal salt marsh, Sci. Total Environ., 686, 1164–1172, https://doi.org/10.1016/j.scitotenv.2019.06.032, 2019.

Carroll, M. A., Heidt, L. E., Cicerone, R. J., and Prinn, R. G.: OCS, H2S, and CS2 fluxes from a salt water marsh, J. Atmos. Chem., 4, 375–395, https://doi.org/10.1007/BF00053811, 1986.

Charlson, R. J., Lovelock, J. E., Andreae, M. O., and Warren, S. G.: Oceanic phytoplankton, atmospheric sulphur, cloud albedo and climate, Nature, 326, 655–661, https://doi.org/10.1038/326655a0, 1987.

Cheng, X., Peng, R., Chen, J., Luo, Y., Zhang, Q., An, S., Chen, J., and Li, B.: CH4 and N2O emissions from Spartina alterniflora and Phragmites australis in experimental mesocosms, Chemosphere, 68, 420–427, https://doi.org/10.1016/J.CHEMOSPHERE.2007.01.004, 2007.

Cooper, D. J., De Mello, W. Z., Cooper, W. J., Zika, R. G., Saltzman, E. S., Prospero, J. M., and Savoie, D. L.: Short-term variability in biogenic sulphur emissions from a Florida Spartina alterniflora marsh, Atmos. Environ., 21, 7–12, 1987a.

Cooper, W. J., Cooper, D. J., Saltzman, E. S., Mello, W. Z. d., Savoie, D. L., Zika, R. G., and Prospero, J. M.: Emissions of biogenic sulphur compounds from several wetland soils in Florida, Atmos. Environ., 21, 1491–1495, https://doi.org/10.1016/0004-6981(87)90311-8, 1987b.

Dacey, J. W. H., King, G. M., and Wakeham, S. G.: Factors controlling emission of dimethylsulphide from salt marshes, Nature, 330, 643–645, https://doi.org/10.1038/330643a0, 1987.

DeLaune, R. D., Devai, I., and Lindau, C. W.: Flux of reduced sulfur gases along a salinity gradient in Louisiana coastal marshes, Estuar. Coast. Shelf Sci., 54, 1003–1011, https://doi.org/10.1006/ecss.2001.0871, 2002.

Diefenderfer, H. L., Cullinan, V. I., Borde, A. B., Gunn, C. M., and Thom, R. M.: High-frequency greenhouse gas flux measurement system detects winter storm surge effects on salt marsh, Glob. Chang. Biol., 24, 5961–5971, https://doi.org/10.1111/gcb.14430, 2018.

DNREC: Delaware National Esturaine Research Reserve Estuarine Profile, 158 pp., 1999.

Duarte, C. M., Middelburg, J. J., and Caraco, N.: Major role of marine vegetation on the oceanic carbon cycle, 2, 1–8, https://doi.org/10.1111/j.2042-7158.1975.tb10261.x, 2005.

Emery, H. E. and Fulweiler, R. W.: Spartina alterniflora and invasive Phragmites australis stands have similar greenhouse gas emissions in a New England marsh, Aquat. Bot., 116, 83–92, https://doi.org/10.1016/j.aquabot.2014.01.010, 2014.

Emmer, I., Needelman, B., Emmett-Mattox, S., Crooks, S., Beers, L., Megonigal, P., Myers, D., Oreska, M., McGlathery, K., and Shoch, D.: Methodology for Tidal Wetland and Seagrass Restoration, 1–115 pp., 2021.

Filippa, G., Cremonese, E., Migliavacca, M., Galvagno, M., Folker, M., Richardson, A. D., and Tomelleri, E.: phenopix: Process Digital Images of a Vegetation Cover, R Packag. version 2.4.2, 2020.

Finster, K., King, G. M., Bak, F., and Finster, K.: Formation of methylmercaptan and dimethylsulfide from methoxylated aromatic compounds in anoxic marine and fresh water sediments, FEMS Microbiol. Ecol., 74, 295–302, https://doi.org/10.1111/j.1574-6968.1990.tb04076.x, 1990.

Goldan, P. D., Kuster, W. C., Albritton, D. L., and Fehsenfeld, F. C.: The measurement of natural sulfur emissions from soils and vegetation: Three sites in the Eastern United States revisited, J. Atmos. Chem., 5, 439–467, https://doi.org/10.1007/BF00113905, 1987.

Granville, K. E., Ooi, S. K., Koenig, L. E., Lawrence, B. A., Elphick, C. S., and Helton, A. M.: Seasonal Patterns of Denitrification and N2O Production in a Southern New England Salt Marsh, 41, 1–13, https://doi.org/10.1007/s13157-021-01393-x, 2021.

Hill, A. C. and Vargas, R.: Methane and Carbon Dioxide Fluxes in a Temperate Tidal Salt Marsh: Comparisons Between Plot and Ecosystem Measurements, J. Geophys. Res. Biogeosciences, 127, e2022JG006943, https://doi.org/10.1029/2022JG006943, 2022.

Hill, A. C., Vázquez-Lule, A., and Vargas, R.: Linking vegetation spectral reflectance with ecosystem carbon phenology in a temperate salt marsh, Agric. For. Meteorol., 307, 108481, https://doi.org/10.1016/j.agrformet.2021.108481, 2021.

Hines, M. E.: Emissions of sulfur gases from wetlands, 25, 153–161, https://doi.org/10.1080/05384680.1996.11904076, 1996.

Järveoja, J., Nilsson, M. B., Gažovič, M., Crill, P. M., and Peichl, M.: Partitioning of the net CO2 exchange using an automated chamber system reveals plant phenology as key control of production and respiration fluxes in a boreal peatland, Glob. Chang. Biol., 24, 3436–3451, https://doi.org/10.1111/gcb.14292, 2018.

Jha, C. S., Rodda, S. R., Thumaty, K. C., Raha, A. K., and Dadhwal, V. K.: Eddy covariance based methane flux in Sundarbans mangroves, India, J. Earth Syst. Sci., 123, 1089–1096, https://doi.org/10.1007/s12040-014-0451-y, 2014.

Jørgensen, B. B. and Okholm-Hansen, B.: Emissions of biogenic sulfur gases from a danish estuary, Atmos. Environ., 19, 1737–1749, https://doi.org/10.1016/0004-6981(85)90001-0, 1985.

Kellogg, W. W., Cadle, R. D., Allen, E. R., Lazrus, A. L., and Martell, E. A.: The Sulfur Cycle, Science (80-.)., 175, 587–596, https://doi.org/10.1016/S0074-6142(08)62696-0, 1972.

Kiene, R. P.: Dimethyl sulfide metabolism in salt marsh sediments, FEMS Microbiol. Lett., 53, 71–78, https://doi.org/10.1016/0378-1097(88)90014-6, 1988.

741 Kiene, R. P. and Visscher, P. T.: Production and fate of methylated sulfur mompounds from
742 methionine and dimethylsulfoniopropionate in anoxic salt marsh sediments, Appl.
743 Environ. Microbiol., 53, 2426–2434, 1987.

744 Kim, J., Verma, S. B., Billesbach, D. P., and Clement, R. J.: Diel variation in methane emission
745 from a midlatitude prairie wetland: Significance of convective throughflow in
746 Phragmites australis, J. Geophys. Res. Atmos., 103, 28029–28039,
747 https://doi.org/10.1029/98JD02441, 1998.

748 Koskinen, M., Minkkinen, K., Ojanen, P., Kämäräinen, M., Laurila, T., and Lohila, A.:
749 Measurements of CO2 exchange with an automated chamber system throughout the
750 year: Challenges in measuring night-time respiration on porous peat soil, 11, 347–363,
751 https://doi.org/10.5194/bg-11-347-2014, 2014.

752 Laursen, A. E. and Seitzinger, S. P.: Measurement of denitrification in rivers: an integrated,
753 whole reach approach, Hydrobiologia, 485, 67–81, 2002.

754 Lin, Y. S., Heuer, V. B., Ferdelman, T. G., and Hinrichs, K.-U.: Microbial conversion of
755 inorganic carbon to dimethyl sulfide in anoxic lake sediment (Plußsee, Germany), 7,
756 2433–2444, https://doi.org/10.5194/bg-7-2433-2010, 2010.

757 Livesley, S. J. and Andrusiak, S. M.: Temperate mangrove and salt marsh sediments are a small
758 methane and nitrous oxide source but important carbon store, Estuar. Coast. Shelf Sci.,
759 97, 19–27, https://doi.org/10.1016/j.ecss.2011.11.002, 2012.

760 Lomans, B. P., Van der Drift, C., Pol, A., and Op den Camp, H. J. M.: Microbial cycling of
761 volatile organic sulfur compounds, Water Sci. Technol., 45, 55–60,
762 https://doi.org/10.1007/s00018-002-8450-6, 2002.

763 Macreadie, P. I., Costa, M. D. P., Atwood, T. B., Friess, D. A., Kelleway, J. J., Kennedy, H.,
764 Lovelock, C. E., Serrano, O., and Duarte, C. M.: Blue carbon as a natural climate
765 solution, Nat. Rev. Earth Environ., 2, 826–839,
766 https://doi.org/https://doi.org/10.1038/s43017-021-00224-1, 2021.

767 McTigue, N. D., Walker, Q. A., and Currin, C. A.: Refining Estimates of Greenhouse Gas
768 Emissions From Salt Marsh “Blue Carbon” Erosion and Decomposition, Front. Mar.
769 Sci., 8, 1–13, https://doi.org/10.3389/fmars.2021.661442, 2021.

770 De Mello, W. Z., Cooper, D. J., Cooper, W. J., Saltzman, E. S., Zika, R. G., Savoie, D. L., and
771 Prospero, J. M.: Spatial and diel variability in the emissions of some biogenic sulfur
772 compounds from a Florida Spartina alterniflora coastal zone, Atmos. Environ., 21, 987–
773 990, https://doi.org/10.1016/0004-6981(87)90095-3, 1987.

774 Middelburg, J. J., Klaver, G., Nieuwenhuize, J., Wielemaker, A., de Hass, W., Vlug, T., and
775 van der Nat, J. F. W. A.: Organic matter mineral sediments along an estuarine gradient,
776 Mar. Ecol. Prog. Ser., 132, 157–168, 1996.

777 Moffett, K. B., Wolf, A., Berry, J. A., and Gorelick, S. M.: Salt marsh-atmosphere exchange of

778 energy, water vapor, and carbon dioxide: Effects of tidal flooding and biophysical
779 controls, 46, https://doi.org/10.1029/2009WR009041, 2010.

780 Möller, I., Kudella, M., Rupprecht, F., Spencer, T., Paul, M., Van Wesenbeeck, B. K., Wolters,
781 G., Jensen, K., Bouma, T. J., Miranda-Lange, M., and Schimmels, S.: Wave attenuation
782 over coastal salt marshes under storm surge conditions, Nat. Geosci., 7, 727–731,
783 https://doi.org/10.1038/NGEO2251, 2014.

784 Moran, J. J., House, C. H., Vrentas, J. M., and Freeman, K. H.: Methyl sulfide production by a
785 novel carbon monoxide metabolism in Methanosarcina acetivorans, Appl. Environ.
786 Microbiol., 74, 540–542, https://doi.org/10.1128/AEM.01750-07, 2008.

787 Morrison, M. C. and Hines, M. E.: The variability of biogenic sulfur flux from a temperate salt
788 marsh on short time and space scales, Atmos. Environ. Part A. Gen. Top., 24A, 1771–
789 1779, https://doi.org/10.1016/0960-1686(90)90509-L, 1990.

790 Moseman-Valtierra, S., Gonzalez, R., Kroeger, K. D., Tang, J., Chao, W. C., Crusius, J.,
791 Bratton, J., Green, A., and Shelton, J.: Short-term nitrogen additions can shift a coastal
792 wetland from a sink to a source of N2O, Atmos. Environ., 45, 4390–4397,
793 https://doi.org/10.1016/j.atmosenv.2011.05.046, 2011.

794 Moseman-Valtierra, S., Abdul-Aziz, O. I., Tang, J., Ishtiaq, K. S., Morkeski, K., Mora, J.,
795 Quinn, R. K., Martin, R. M., Egan, K., Brannon, E. Q., Carey, J., and Kroeger, K. D.:
796 Carbon dioxide fluxes reflect plant zonation and belowground biomass in a coastal
797 marsh, 7, e01560, 2016.

798 Murray, R. H., Erler, D. V., and Eyre, B. D.: Nitrous oxide fluxes in estuarine environments :
799 response to global change, Glob. Chang. Biol., 21, 3219–3245,
800 https://doi.org/10.1111/gcb.12923, 2015.

801 Van Der Nat, F. and Middelburg, J. J.: Methane emission from tidal freshwater marshes,
802 Biogeochemistry, 49, 103–121, 2000.

803 Neubauer, S. C. and Megonigal, J. P.: Correction to: Moving Beyond Global Warming
804 Potentials to Quantify the Climatic Role of Ecosystems, Ecosyst. 2019 228, 22, 1931–
805 1932, https://doi.org/10.1007/S10021-019-00422-5, 2019.

806 System-wide Monitoring Program:

807 Oremland, R. S., Marsh, L. M., and Polcin, S.: Methane production and simultaneous sulphate
808 reduction in anoxic, salt marsh sediments, Nature, 296, 143–145, 1982.

809 Peterson, P. M., Romaschenko, K., Arrieta, Y. H., and Saarela, J. M.: A molecular phylogeny
810 and new subgeneric classification of Sporobolus (Poaceae: Chloridoideae:
811 Sporobolinae), Taxon, 63, 1212–1243, https://doi.org/10.12705/636.19, 2014.

812 Petrakis, S., Seyfferth, A., Kan, J., Inamdar, S., and Vargas, R.: Influence of experimental
813 extreme water pulses on greenhouse gas emissions from soils, Biogeochemistry, 133,

147–164, https://doi.org/10.1007/s10533-017-0320-2, 2017.

Rinne, J., Riutta, T., Pihlatie, M., Aurela, M., Haapanala, S., Tuovinen, J. P., Tuittila, E. S., and Vesala, T.: Annual cycle of methane emission from a boreal fen measured by the eddy covariance technique, Tellus, Ser. B Chem. Phys. Meteorol., 59, 449–457, https://doi.org/10.1111/j.1600-0889.2007.00261.x, 2007.

Rosentreter, J. A., Maher, D. T., Erler, D. V., Murray, R. H., and Eyre, B. D.: Methane emissions partially offset "blue carbon" burial in mangroves, Sci. Adv., 4, eaao4985, https://doi.org/10.1126/SCIADV.AAO4985, 2018.

Rosentreter, J. A., Al-Haj, A. N., Fulweiler, R. W., and Williamson, P.: Methane and Nitrous Oxide Emissions Complicate Coastal Blue Carbon Assessments, Global Biogeochem. Cycles, 35, e2020GB006858, https://doi.org/10.1029/2020GB006858, 2021.

Savage, K., Phillips, R., and Davidson, E.: High temporal frequency measurements of greenhouse gas emissions from soils, 11, 2709–2720, https://doi.org/10.5194/bg-11-2709-2014, 2014.

Sela-Adler, M., Said-Ahmad, W., Sivan, O., Eckert, W., Kiene, R. P., and Amrani, A.: Isotopic evidence for the origin of dimethylsulfide and dimethylsulfoniopropionate-like compounds in a warm, monomictic freshwater lake, Environ. Chem., 13, 340–351, https://doi.org/https://doi.org/10.1071/EN15042, 2015.

Seyednasrollah, B., Young, A. M., Hufkens, K., Milliman, T., Friedl, M. A., Frolking, S., Richardson, A. D., Abraha, M., Allen, D. W., Apple, M., Arain, M. A., Baker, J., Baker, J. M., Baldocchi, D., Bernacchi, C. J., Bhattacharjee, J., Blanken, P., Bosch, D. D., Boughton, R., Boughton, E. H., and Zona, D.: PhenoCam dataset v2.0: Vegetation phenology from digital camera imagery, Oak Ridge, Tennessee, https://doi.org/https://doi.org/10.3334/ ORNLDAAC/1674, 2019.

Seyfferth, A. L., Bothfeld, F., Vargas, R., Stuckey, J. W., Wang, J., Kearns, K., Michael, H. A., Guimond, J., Yu, X., and Sparks, D. L.: Spatial and temporal heterogeneity of geochemical controls on carbon cycling in a tidal salt marsh, Geochim. Cosmochim. Acta, 282, 1–18, https://doi.org/10.1016/j.gca.2020.05.013, 2020.

Simpson, L. T., Osborne, T. Z., and Feller, I. C.: Wetland Soil CO2 Efflux Along a Latitudinal Gradient of Spatial and Temporal Complexity, 42, 45–54, https://doi.org/10.1007/s12237-018-0442-3, 2019.

Steudler, P. A. and Peterson, B. J.: Contribution of gaseous sulphur from salt marshes to the global sulphur cycle, Nature, 311, 455–457, https://doi.org/10.1038/311455a0, 1984.

Steudler, P. A. and Peterson, B. J.: Annual cycle of gaseous sulfur emissions from a New England Spartina alterniflora marsh, Atmos. Environ., 19, 1411–1416, https://doi.org/10.1016/0004-6981(85)90278-1, 1985.

Taubman, S. J. and Kasting, J. F.: Carbonyl sulfide: No remedy for global warming, Geophys.

Res. Lett., 22, 803–805, https://doi.org/10.1029/95GL00636, 1995.

Thomas, M. A., Suntharalingam, P., Pozzoli, L., Rast, S., Devasthale, A., Kloster, S., Feichter, J., and Lenton, T. M.: Quantification of DMS aerosol-cloud-climate interactions using the ECHAM5-HAMMOZ model in a current climate scenario, Atmos. Chem. Phys., 10, 7425–7438, https://doi.org/10.5194/acp-10-7425-2010, 2010.

Tong, C., Huang, J. F., Hu, Z. Q., and Jin, Y. F.: Diurnal Variations of Carbon Dioxide, Methane, and Nitrous Oxide Vertical Fluxes in a Subtropical Estuarine Marsh on Neap and Spring Tide Days, 36, 633–642, https://doi.org/10.1007/s12237-013-9596-1, 2013.

Tong, C., Morris, J. T., Huang, J., Xu, H., and Wan, S.: Changes in pore-water chemistry and methane emission following the invasion of Spartina alterniflora into an oliogohaline marsh, Limnol. Oceanogr., 63, 384–396, https://doi.org/10.1002/lno.10637, 2018.

Trifunovic, B., Vázquez-Lule, A., Capooci, M., Seyfferth, A. L., Moffat, C., and Vargas, R.: Carbon Dioxide and Methane Emissions From Temperate Salt Marsh Tidal Creek, J. Geophys. Res. Biogeosciences, 125, https://doi.org/10.1029/2019JG005558, 2020.

Turetsky, M. R., Kotowska, A., Bubier, J., Dise, N. B., Crill, P., Hornibrook, E. R. C., Minkkinen, K., Moore, T. R., Myers-Smith, I. H., Nykanen, H., Olefeldt, D., Rinne, J., Saarnio, S., Shurpali, N., Tuittila, E. S., Waddington, J. M., White, J. R., Wickland, K. P., and Wilmking, M.: A synthesis of methane emissions from 71 northern, temperate, and subtropical wetlands, Glob. Chang. Biol., 20, 2183–2197, https://doi.org/10.1111/gcb.12580, 2014.

UNFCCC: Paris Agreement, 2015.

Vargas, R., Carbone, M. S., Reichstein, M., and Baldocchi, D. D.: Frontiers and challenges in soil respiration research: from measurements to model-data integration, Biogeochemistry, 102, 1–13, https://doi.org/10.1007/s10533-010-9462-1, 2011.

Vázquez-Lule, A. and Vargas, R.: Biophysical drivers of net ecosystem and methane exchange across phenological phases in a tidal salt marsh, Agric. For. Meteorol., 300, https://doi.org/10.1016/j.agrformet.2020.108309, 2021.

Wang, J. and Wang, J.: Spartina alterniflora alters ecosystem DMS and CH4 emissions and their relationship along interacting tidal and vegetation gradients within a coastal salt marsh in Eastern China, Atmos. Environ., 167, 346–359, https://doi.org/10.1016/J.ATMOSENV.2017.08.041, 2017.

Ward, N., Megonigal, P. J., Bond-Lamberty, B., Bailey, V., Butman, D., Canuel, E., Diefenderfer, H., Ganju, N. K., Goñi, M. A., Graham, E. B., Hopkinson, C. S., Khangaonkar, T., Langley, J. A., McDowell, N. G., Myers-Pigg, A. N., Neumann, R. B., Osburn, C. L., Price, R. M., Rowland, J., Sengupta, A., Simard, M., Thornton, P. E., Tzortziou, M., Vargas, R., Weisenhorn, P. B., and Windham-Myers, L.: Representing the Function and Sensitivity of Coastal Interfaces in Earth System Models, Nat. Commun., 11, https://doi.org/10.1038/s41467-020-16236-2, 2020.

Watts, S. F.: The mass budgets of carbonyl sulfide, dimethyl sulfide, carbon disulfide and hydrogen sulfide, Atmos. Environ., 34, 761–779, https://doi.org/10.1016/S1352-2310(99)00342-8, 2000.

Whelan, M. E., Min, D. H., and Rhew, R. C.: Salt marsh vegetation as a carbonyl sulfide (COS) source to the atmosphere, Atmos. Environ., 73, 131–137, https://doi.org/10.1016/J.ATMOSENV.2013.02.048, 2013.

Wilson, B. J., Mortazavi, B., and Kiene, R. P.: Spatial and temporal variability in carbon dioxide and methane exchange at three coastal marshes along a salinity gradient in a northern Gulf of Mexico estuary, Biogeochemistry, 123, 329–347, https://doi.org/10.1007/s10533-015-0085-4, 2015.

Xie, H. and Moore, R. M.: Carbon disulfide in the North Atlantic and Pacific Oceans, J. Geophys. Res. Ocean., 104, 5393–5402, https://doi.org/10.1029/1998jc900074, 1999.

Xie, X., Zhang, M.-Q., Zhao, B., and Guo, H.-Q.: Dependence of coastal wetland ecosystem respiration on temperature and tides: a temporal perspective, 11, 539–545, https://doi.org/10.5194/bg-11-539-2014, 2014.

Xu, X., Fu, G., Zou, X., Ge, C., and Zhao, Y.: Diurnal variations of carbon dioxide, methane, and nitrous oxide fluxes from invasive Spartina alterniflora dominated coastal wetland in northern Jiangsu Province, Acta Oceanol. Sin., 36, 105–113, https://doi.org/10.1007/s13131-017-1015-1, 2017.

Yang, W.-B., Yuan, C.-S., Huang, B.-Q., Tong, C., and Yang, L.: Emission Characteristics of Greenhouse Gases and Their Correlation with Water Quality at an Estuarine Mangrove Ecosystem – the Application of an In-situ On-site NDIR Monitoring Technique, Wetl. 2018 384, 38, 723–738, https://doi.org/10.1007/S13157-018-1015-8, 2018.

Yang, W.-B. Bin, Yuan, C.-S. S., Tong, C., Yang, P., Yang, L., and Huang, B.-Q. Q.: Diurnal variation of CO2, CH4, and N2O emission fluxes continuously monitored in-situ in three environmental habitats in a subtropical estuarine wetland, Mar. Pollut. Bull., 119, 289–298, https://doi.org/10.1016/j.marpolbul.2017.04.005, 2017.

Yu, X., Ye, S., Olsson, L., Wei, M., Krauss, K. W., and Brix, H.: A 3-Year In-Situ Measurement of CO 2 Efflux in Coastal Wetlands: Understanding Carbon Loss through Ecosystem Respiration and its Partitioning, https://doi.org/10.1007/s13157-019-01197-0, 2019.

Yu, Z., Li, Y., Deng, H., Wang, D., Chen, Z., and Xu, S.: Effect of Scirpus mariqueter on nitrous oxide emissions from a subtropical monsoon estuarine wetland, J. Geophys. Res. Biogeosciences, 117, 2017, https://doi.org/10.1029/2011JG001850, 2012.

Zhang, Y. and Ding, W.: Diel methane emissions in stands of Spartina alterniflora and Suaeda salsa from a coastal salt marsh, Aquat. Bot., 95, 262–267, https://doi.org/10.1016/j.aquabot.2011.08.005, 2011.

926 Zhang, Y., Wang, L., Xie, X., Huang, L., and Wu, Y.: Effects of invasion of Spartina
927 alterniflora and exogenous N deposition on N2O emissions in a coastal salt marsh, Ecol.
928 Eng., 58, 77–83, https://doi.org/10.1016/j.ecoleng.2013.06.011, 2013.

929